

Control of the waveform dispersion effect and applications in a TEM imaging technique for identifying underground objects

This content has been downloaded from IOPscience. Please scroll down to see the full text.

2011 J. Geophys. Eng. 8 195

(<http://iopscience.iop.org/1742-2140/8/2/007>)

View [the table of contents for this issue](#), or go to the [journal homepage](#) for more

Download details:

IP Address: 141.219.24.186

This content was downloaded on 12/05/2014 at 18:20

Please note that [terms and conditions apply](#).

Control of the waveform dispersion effect and applications in a TEM imaging technique for identifying underground objects

G Q Xue¹, Y J Yan^{2,4} and X Li³

¹ Institute of Geology and Geophysics Academic, Chinese Academy of Sciences, Beijing, 100029, People's Republic of China

² Department of Engineering Mechanics, Northwestern Polytechnical University, Xi'an, 710072, People's Republic of China

³ College of Geology Engineering and Geomatics, Chang'an University, 710054, Xi'an, People's Republic of China

E-mail: yjyan_2895@nwpu.edu.cn

Received 17 September 2010

Accepted for publication 17 January 2011

Published 10 March 2011

Online at stacks.iop.org/JGE/8/195

Abstract

The pseudo-seismic waves obtained by the transient electromagnetic method (TEM) can be used to explain geological conformations of underground objects. However, the directly transformed pseudo-wave always has a dispersive and broader waveform so that it cannot clearly indicate the geological–electrical boundary of the explored underground objects. This study shows that the reason for the waveform dispersion is because the variance of the kernel function with the Gauss distribution is the real time; the wave distribution range will increase with increasing time. Therefore, this study presents a technique for enhancing the resolving power of pseudo-seismic data processed by a de-convolution method, and detailed theory and algorithms are reported. The pseudo-seismic signals of two geological–electrical models are taken as the examples to verify the present algorithm. Results show that the pseudo-seismic waves after de-convolution processes have sharper waveforms and narrower distribution zones, and this can effectively control the waveform broadening phenomenon and is able to enhance the resolving power using the TEM pseudo-seismic waves to survey the boundary of underground objects.

Keywords: transient electromagnetic field, pseudo-seismic wave, waveform dispersion, de-convolution, geological–electrical interfaces

1. Introduction

A transient electromagnetic method (TEM) has been widely used in complex geological exploration, and also the inverse algorithms of the TEM have been developed (Auken *et al* 2003, Ranieri *et al* 2005). With the increasing demand of fine exploration in many engineering industries, the existing inversion algorithms of the TEM cannot meet the practical

requirements in a large number of geological surveys, so the method of pseudo-seismic imaging has been put forward and it has become a hot topic in the TEM application. The main process of the pseudo-seismic imaging technique is to transform the TEM data into plane wave data; then based on the idea of pseudo-seismic data analogous to magnetotelluric (MT) data, a pseudo-seismic image is obtained using a series of reflection coefficients, but the resolving power of the technique directly using TEM data is not sufficient for meeting the needs

⁴ Author to whom any correspondence should be addressed.

of identifying underground objects in a geological survey. In order to solve this problem, according to the comparability between the wave equation in non-dissipative media and the diffusion equation in highly conductive media, Lee *et al* (1989) first presented the transform formula of both, i.e. the wave field transformation form of the electromagnetic wave fields between the above two media. Subsequently, this analogous method of explaining seism using the TEM was applied to the geological survey (Gershenson 1997, Lee *et al* 2002).

In the seismology field, there have been many research experiments on the resolution of seismic waves. Denham and Sheriff (1980) gave a comprehensive review of the constraint factors of the resolution for the central and offset seismic section planes. Safar (1985) discussed the factors of influencing transverse resolution through the offset of the integral method based on point scatters. Wu and Toksoz (1987) used the seismic tomography imagery and multi-source information geology display to study the relationships between the resolution of space imaging and the coverage region of spatial frequency. In most cases, the seismic wavelet can be compressed into narrow pulses through de-convolution so that the resolution of seismic waves can be improved. Although the electromagnetic response field can be transformed into pseudo-seismic waves (Xue *et al* 2007), the research on the resolution of the electromagnetic survey was scarcely reported because of the complicated nature of the electromagnetic response field. The propagating speed of such pseudo-seismic waves depends not only on the conductivity of the detected media, but also on the conductivity of adjacent media, so this is very different from the real seismic wave field. A harmful problem caused by this essential difference is the wave dispersion effect, which will decrease the resolution of the obtained imaginary wave field data. This will be a great drawback in the interpretation of the pseudo-TEM method.

Obviously, the wave dispersion effect will greatly influence the space imaging quality of the TEM and limit the TEM application in geological surveys. Therefore, it is necessary to explore the origin of the wave dispersion effect and control this wave dispersion.

This study first discusses the dispersion origin of the imaginary waveform, and confirms that the wave dispersion is not produced by the energy loss while propagating through the media, but is caused by the increase of the distribution range in the kernel function of the Gauss distribution with the imaginary time range in the wave transformation. Then, the control method for the wave dispersion effect is constructed through computing the de-convolution of the sampled data of pseudo-TEM. Finally, based on the calculation validation of a theoretical model, the results show that the present method can control the wave dispersion. Thus, the improved method can enhance the ability of the pseudo-seismic imaging method to distinguish underground electrical boundaries so that the 3D interpretation of TEM can be realized.

2. Waveform dispersion effect and its origin

Based on the transform relationship between the pseudo-seismic wave field and the electric-field intensity, which

satisfies the diffusion equation in the time domain, the relationship between the pseudo-seismic wave field and the time domain transient response of the large-loop source according to the Maxwell equation can be expressed as

$$H_m(t) = \frac{1}{2\sqrt{\pi t^3}} \int_0^\infty \tau e^{-\frac{\tau^2}{4t}} U(\tau) d\tau \quad (1)$$

where the variable τ is the square root of the time variable t , $U(\tau)$ is the pseudo-seismic wave field function with the wave speed $1/\sqrt{\mu\sigma}$, and $H_m(t)$ is the diffusion field of transient response in a time domain.

Traditionally, equation (1) is called the positive problem. In contrast, it is called the inverse problem if one wants to calculate the pseudo-seismic wave field $U(\tau)$ based on the known time domain response $H_m(t)$. We successfully solved this inverse transform through the combined bi-optimization and regularization algorithm (Xue *et al* 2006).

In the course in which the transient electromagnetic field is transformed into the pseudo-seismic wave field, the waveform of the obtained pseudo-seismic wave field will broaden with increasing time, which will execrably influence the imaging resolution. In fact, this phenomenon can be explained through the characteristics of the kernel function $a(t, \tau)$ used in the wave field transform. This kernel function $a(t, \tau)$ follows as

$$a(t, \tau) = \frac{1}{2\sqrt{\pi t^3}} \tau e^{-\frac{\tau^2}{4t}}. \quad (2)$$

Obviously, the variance of the kernel function with the Gauss distribution is the real time, and the ending time of its time domain increases with increasing time, so the wave field form becomes more dispersive.

Although the waveform dispersion is caused by the mathematical transform, this is similar to the action of the earth filter (low-pass) in a seismic survey. From the filtering wave point of view, if one wants to enhance the resolving power of a seismic survey, it can be actualized through the de-convolution algorithm, which can eliminate the action of the earth filter by searching for an anti-filtering factor. It has been theoretically and practically proved that the energy of the dispersion waves can be concentrated so that finer resolution is attainable (Snieder *et al* 2006).

In order to explain the increase in the extent of wave distribution in the kernel function with increasing time, the distribution configuration variations of the kernel function value with imaginary time τ at different time points are shown in figure 1. It can be seen from figure 1 that the distribution range of the kernel function $a(t, \tau)$ obviously becomes broader with imaginary time τ , and this will result in a wave dispersion of the pseudo-seismic wave field with time extending after the inverse transform. Besides, the electromagnetic wave speed is $c_0 = 1/\sqrt{\mu_0\epsilon_0}$ in free space, while the imaginary wave speed is $v = 1/\sqrt{\mu_0\sigma}$ in non-dissipative media. Quantitatively, v is smaller than c_0 , and this indicates that, if propagating distance in the imaginary non-dissipative media, the pseudo-seismic wave needs more time; therefore, this will result in more remarkable waveform dispersion.

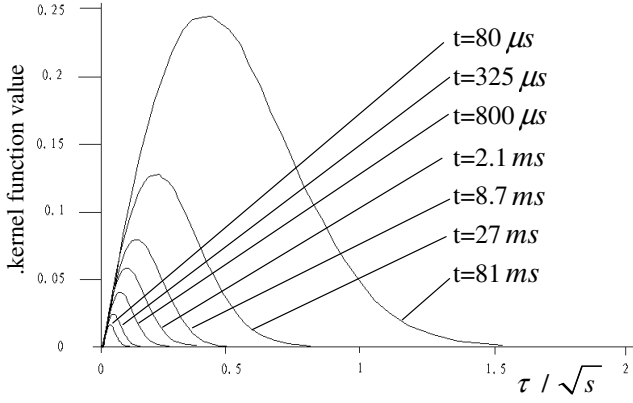


Figure 1. Distribution natures of the kernel function.

3. Control and compression of waveform dispersion based on de-convolution

In the seismic geology survey, the sharp pulse series indicating the stratigraphic sequence are often blurred because of the filtering action of the earth and noise disturbance; thus, the resolving power of stratigraphic structures is badly weakened. At present, the technique for enhancing the resolving power of processing seismic data by the de-convolution method is being widely used (Parolai *et al* 2009). Similarly, this can also be applied to process the pseudo-seismic wave in the TEM.

Assuming that $\mathbf{y}(t)$ is a transformed pseudo-seismic wave, $\mathbf{y}(t) = \{y_0, y_1, y_2, \dots, y_n\}$, we can use a filter $h(t) = \{h_0, h_1, h_2, \dots, h_m\}$ to filter $\mathbf{y}(t)$ to obtain

$$\hat{y}(t) = y(t) * h(t) = \sum_{\tau=0}^m h(\tau)y(t - \tau) \quad (3)$$

where $\hat{y}(t)$ is the pseudo-seismic wave after filtering.

If the expected filter output is $\tilde{y}(t) = \{\tilde{y}_0, \tilde{y}_1, \tilde{y}_2, \dots, \tilde{y}_{m+n}\}$, then the error square sum Q of the practical output $\hat{y}(t)$ and the expected filter output $\tilde{y}(t)$ can be expressed as

$$Q = \sum_{t=0}^{m+n} [\hat{y}(t) - \tilde{y}(t)]^2 = \sum_{t=0}^{m+n} \left[\sum_{\tau=0}^m h(\tau)y(t - \tau) - \tilde{y}(t) \right]^2. \quad (4)$$

If we hope that Q should be minimum through selecting an appropriate filter $h(t)$, one can obtain

$$\frac{\partial Q}{\partial h(k)} = 2 \sum_{t=0}^{m+n} \left(\sum_{\tau=0}^m h(\tau)y(t - \tau) - \tilde{y}(t) \right) y(t - k) = 0. \quad (5)$$

Equation (5) is also written as

$$\sum_{\tau=0}^m h(\tau) \sum_{t=0}^{m+n} y(t - \tau)y(t - k) = \sum_{t=0}^{m+n} \tilde{y}(t)y(t - k), \quad k = 1, 2, \dots, m. \quad (6)$$

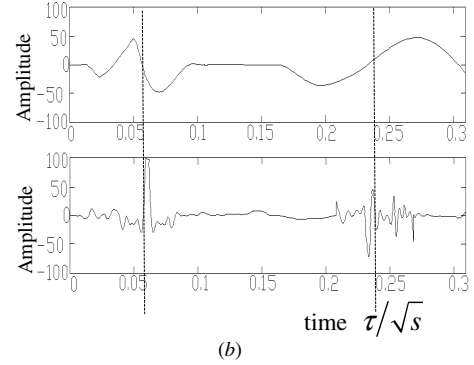
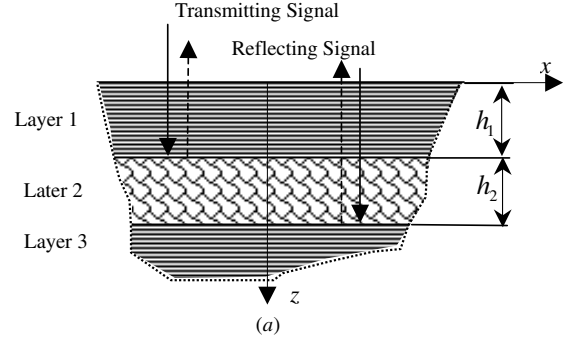


Figure 2. Geological model and comparison of its pseudo-seismic waves before and after de-convolution processing. (a) Geological structural model with three layers. (b) Waveform before and after de-convolution processing.

Let

$$\sum_{t=0}^{m+n} y(t - \tau)y(t - k) = r_{yy}(\tau - k) \quad (7)$$

$$\sum_{t=0}^{m+n} \tilde{y}(t)y(t - k) = r_{\tilde{y}y}(k). \quad (8)$$

Obviously, $r_{yy}(\tau - k)$ is the autocorrelation function of the pseudo-seismic wave $y(t)$ at the time delay $\tau - k$, and the $r_{\tilde{y}y}(k)$ is the cross correlation function of $y(t)$ and the expected filter output $\tilde{y}(t)$ at the time delay k . Thus, equation (6) can be written as

$$\sum_{\tau=0}^m r_{yy}(\tau - k)h(\tau) = r_{\tilde{y}y}(k), \quad k = 0, 1, 2, \dots, m. \quad (9)$$

Equation (9) can also be expressed as the following matrix equation:

$$\begin{bmatrix} r_{yy}(0) & r_{yy}(1) & \cdots & r_{yy}(m) \\ r_{yy}(1) & r_{yy}(0) & \cdots & r_{yy}(m-1) \\ \vdots & \vdots & \ddots & \vdots \\ r_{yy}(m) & r_{yy}(m-1) & \cdots & r_{yy}(0) \end{bmatrix} \begin{bmatrix} h(0) \\ h(1) \\ \vdots \\ h(m) \end{bmatrix} = \begin{bmatrix} r_{\tilde{y}y}(0) \\ r_{\tilde{y}y}(1) \\ \vdots \\ r_{\tilde{y}y}(m) \end{bmatrix}. \quad (10)$$

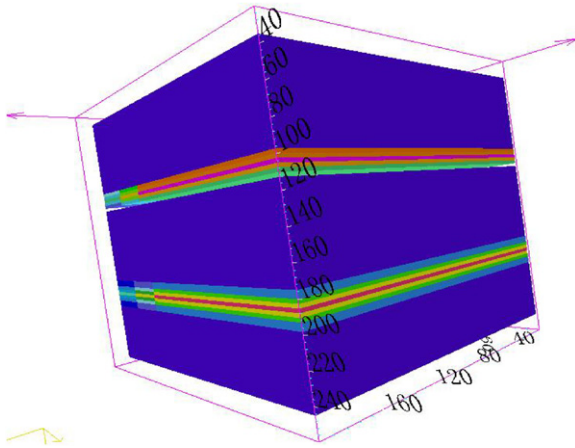


Figure 3. Image of the geological model based on the compressed pseudo-seismic wave.

To solve equation (10), one should obtain the required filter factor $h(t)$. Then, the filtered pseudo-seismic wave $\hat{y}(t)$ can be calculated using equation (3).

Theoretically, the length of the filtering factor can be discretionarily selected. Usually, its length is selected to be 80, 120, 160, 200 or 240 ms in seismic exploration. However,

the length of the filtering factor must be converted into the number of samples, so the length should be selected according to the total number of data after interpolation. Only when the length is appropriate, does the de-convolution effect become stable. In this study, the length of the de-convolution filter is selected to be 400–600 ms.

4. Experiments and simulation validations on geological models

A geological model with three layers being used for the TEM survey is shown in figure 2(a), and the thicknesses of its first and second layers are $h_1 = h_2 = 100$ m. The resistivities of the first, second and third layers are $\rho_1 = 100 \Omega \text{ m}$, $\rho_2 = 5 \Omega \text{ m}$ and $\rho_3 = 100 \Omega \text{ m}$, respectively. The upper wave in figure 2(b) is the pseudo-seismic wave obtained using the transient electromagnetic method for the upper side of the object layer 2. Through the peak, the wave signal can indicate the boundary of an underground object; this kind of indication in the upper wave in figure 2(b) is inexplicable because the waveform of the pseudo-seismic wave is dispersive and has lower resolution. This shows that the identification of the underground object directly using the pseudo-seismic wave obtained by the TEM is often inaccurate if the wave signal is not correctly processed. Using the de-convolution method

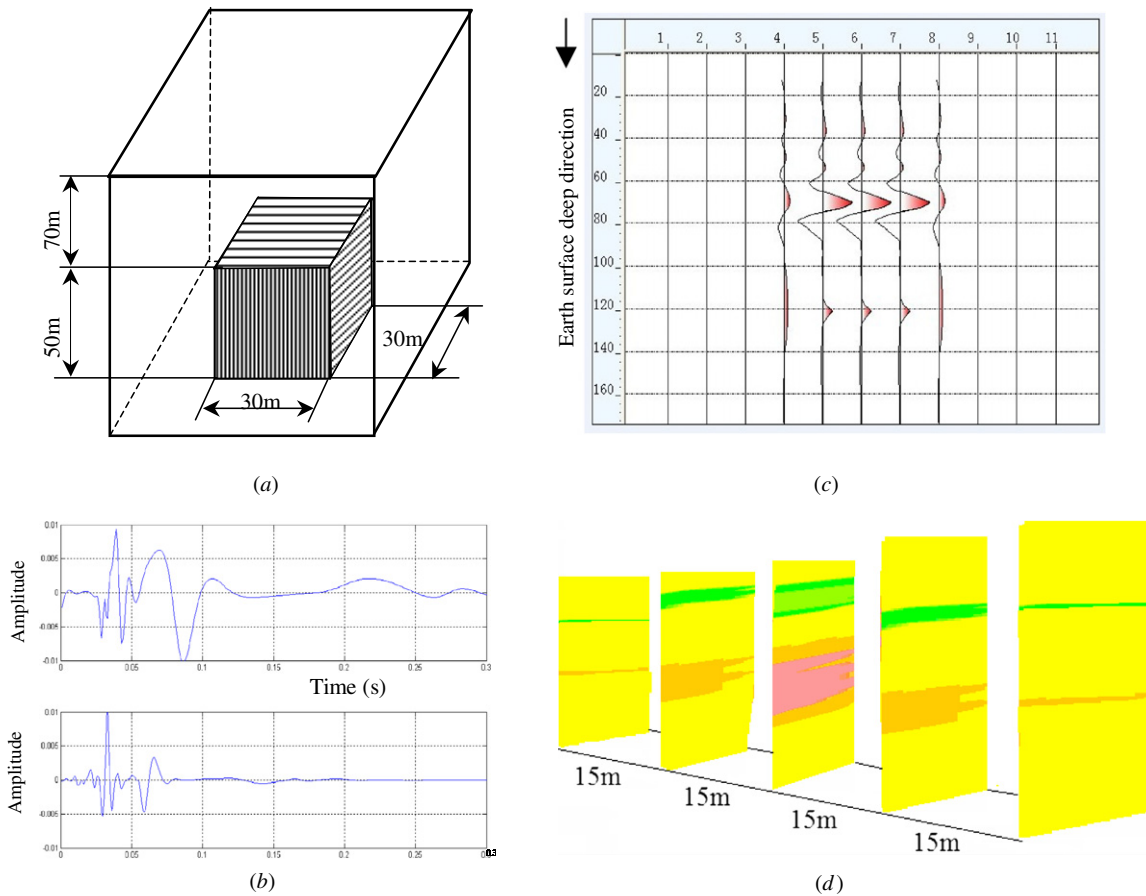


Figure 4. Three-dimensional geological model and its pseudo-seismic wave before and after de-convolution processing. (a) The geological model of three dimensions. (b) Waveform before and after de-convolution processing. (c) Geological imaging section of the compressed pseudo-seismic wave. (d) Edge effect of the transformed wave.

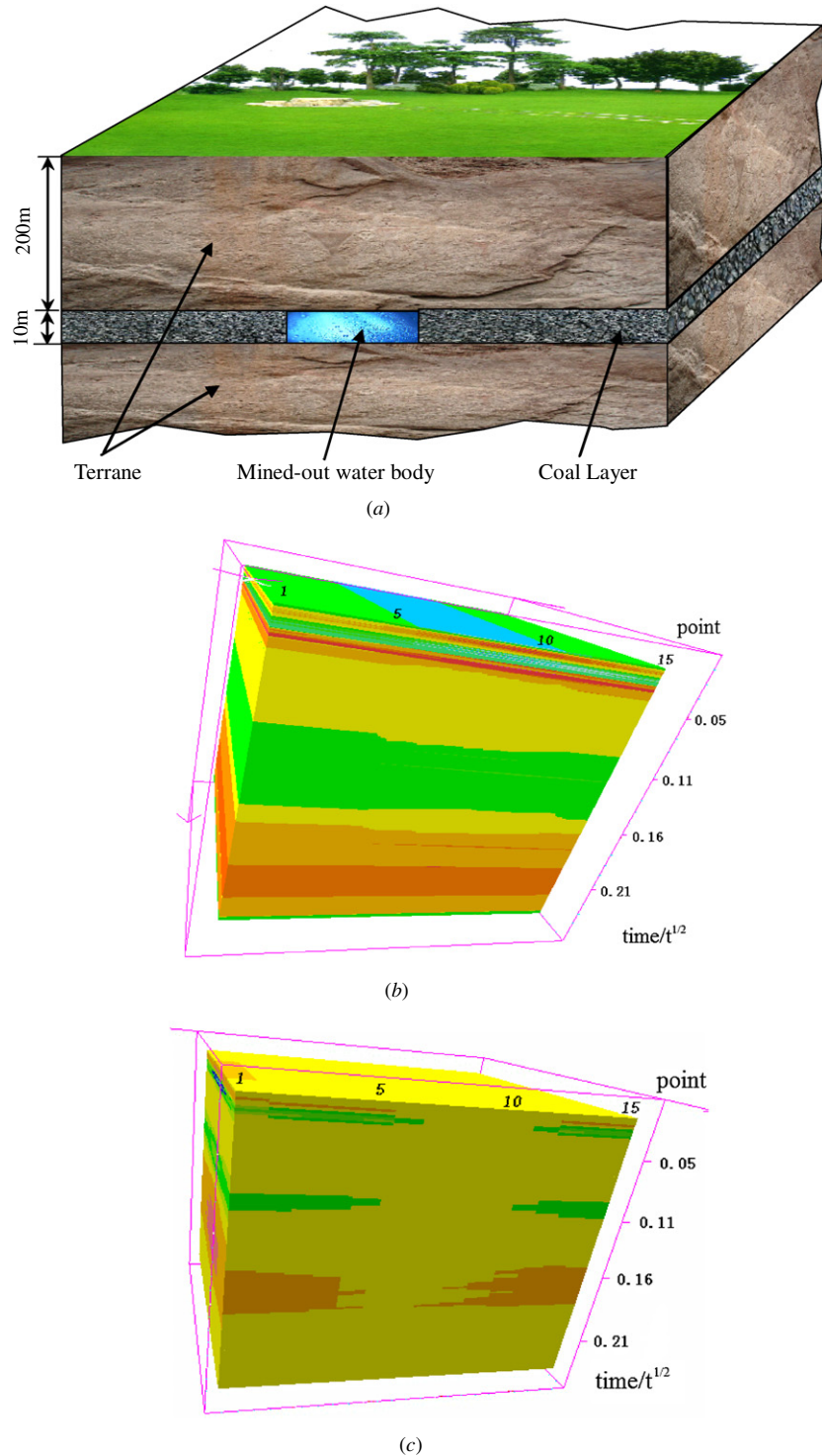


Figure 5. The geological–electrical model of a mined-out area and the edge effect of the transformed wave field. (a) Geological–electrical model of a mined-out area. (b) Result of the transformed wave field without wave compression. (c) Result of the transformed wave field with wave compression.

given in section 3 to control and compress the waveform in the upper wave in figure 2(b), one can obtain the finer wave with the obvious mutation and the narrow pulse waves shown as the lower wave in figure 2(b). It can be seen that the waveform after the de-convolution process is compressed and sharpened so that the boundaries of the geological–electrical layers are clearer. This indicates that the de-convolution process on the

pseudo-seismic wave can greatly enhance the resolving power of the reflecting signals.

In order to check the real effect of exploring the geological structure shown in figure 2(a) using the de-convolution technique, the geological images of the model constructed using the pseudo-seismic wave after the de-convolution process are shown in figure 3. It is seen that the wave

energy produced by the upper geological–electrical interface concentrates at approximately 100 m, and the wave energy produced by the deeper interface centralizes between 190 and 200 m. This is accordant with the real positions 100 and 200 m of the practical geological interfaces of the model.

On the other hand, a more complex geological–electrical model with 3D (shown in figure 4(a)) is presented for validating the control effect of the pseudo-seismic wave using the de-convolution algorithm. The resistivity of the half space model is $\rho_1 = 10 \Omega \text{ m}$, and its dimensions are $100 \text{ m} \times 100 \text{ m} \times 170 \text{ m}$. The explored object is buried under 70 m depth, its dimensions are $30 \text{ m} \times 30 \text{ m} \times 50 \text{ m}$, and its resistivity is $\rho_2 = 300 \Omega \text{ m}$.

The upper wave in figure 4(b) is the pseudo-seismic wave obtained using the transient electromagnetic method for the explored object, and the lower wave in figure 4(b) is the wave signal after the de-convolution processing. One can find that the pseudo waveform directly obtained by the TEM is relatively wide near the reflected boundary and hence the resolution is lower, and the controlled and compressed waveform after de-convolution has a great and narrow wave peak. Obviously, the waveform near the geological–electrical boundary can be sharpened or energy centralized, and the more controlled data also indicate that the wave energy of the up-boundary focuses at the depth of 70 m, and that of the down-boundary mainly focuses at the depth of 120 m.

In fact, the wave dispersion effect is more severe for the lower interface of the explored object because the reflection from high resistance to low resistance is a weak reflecting interface. However, the waveform after the de-convolution processing will be able to indicate this geological–electrical boundary as shown in figure 4(c). In order to display the resolution of the transformed wave, its sections every 15 m are shown in figure 4(d). For the middle sections, the edges of the transformed wave are clear and in accordance with the positions of the detected object. However, section edges near the two side boundaries of the surveyed object gradually become unclear. This indicates that there is indeed a transverse edge effect.

In order to indicate that the method proposed in this study can improve the edge effect, a more complicated geological–electrical model, which includes a mined-out water body shown in figure 5(a), is used to demonstrate resolution improvement. The model is composed of three layers: the first layer with the thickness of 100 m is terrane with the resistivity of $100 \Omega \text{ m}$, the second layer with the thickness 10 m is composed of coal with the resistivity of $200 \Omega \text{ m}$ and water with the resistivity of $30 \Omega \text{ m}$, and the third layer is also terrane with the resistivity of $100 \Omega \text{ m}$.

The results of the transformed wave fields without and with wave compression are given in figures 5(b) and (c), respectively. In figure 5(b), one can find that, although the leaps of upper and lower two waves can be identified, the leaps are not clear enough. Simultaneously, the boundary between mined-out water and coal in the interlayer is very fuzzy. However, when the transformed wave field is processed by the proposed method, the image obtained in figure 5(c) can clearly indicate the leaps of upper and lower two waves because

the width of sub-waves is narrow and the layered interface is also very clear. In addition, the edges of the water structure are clearer, and this shows that the resolutions in transverse and lengthway directions have been greatly improved after the data were processed by the proposed method. Especially, one can identify the coal and mined-out layers from the image shown in figure 5(c), and this indicates that the boundaries of coal and mined-out area can also be differentiated through the proposed method.

5. Conclusions

The transform relationship between the diffusion equation of the electromagnetic field of a conductive media and the non-damped wave equation of a non-dissipative medium can be used to implement the pseudo-seismic data analysis of the TEM. Its principle is to extract the characteristics of transient electromagnetic response related to wave propagation for the explored underground objects. However, the directly transformed pseudo-wave always has a dispersive and broad waveform so that it cannot clearly indicate the geological–electrical boundary of the explored underground objects. This study shows that the reason for the waveform broadening is not energy loss in the wave propagation, but is the kernel function of wave field transformation. Because the variance of the kernel function with the Gauss distribution is in real time, its distribution range will increase with increasing time. The longer the time, the broader the waveform will be. Therefore, this study presents a technique for enhancing the resolving power of processing pseudo-seismic data by the de-convolution method, and detailed theory and algorithm are reported.

Three geological–electrical models to be explored are given, and their pseudo-seismic signals are experimentally obtained based on the TEM. Results show that the pseudo-seismic waves after de-convolution processes have sharper waveform and narrower distribution zone. This testifies that the de-convolution method can effectively control the waveform broadening phenomenon and is able to enhance the resolving power using the TEM pseudo-seismic waves to survey the boundary of an underground object.

Acknowledgments

The authors would like to thank the Natural Science Foundation of China for support under the grants 40774066 and Major Program of the Natural Science Foundation of China under the grants 50539080, and Knowledge Innovation Project of The Chinese Academic of Sciences under the grants KZCX2-YW-Q04-07.

References

- Auken E, Jorgensen F and Sorensen K I 2003 Large-scale TEM investigation for ground-water *Explor. Geophys.* **34** 188–94
- Denham L R and Sheriff R E 1980 What is horizontal resolution? Expanded Abstract of *50th Annual Int. SEG Meeting, Session G17*

- Gershenson M 1997 Simple interpretation of time domain electromagnetic sounding using similarities between wave and diffusion propagation *Geophysics* **62** 763–74
- Lee K H, Liu G and Morrison H F 1989 A new approach to modeling the electromagnetic response of conductive media *Geophysics* **54** 1180–92
- Lee T J, Suh J H, Kim H J, Song Y and Lee K H 2002 Electromagnetic travel time tomograph using approxobility wave-field transform *Geophysics* **67** 68–76
- Parolai S, Ansal A, Kurtulus A, Strollo A, Wang R J and Zschau J 2009 The Atakoy vertical array (Turkey): insights into seismic wave propagation in the shallow-most crustal layers by waveform deconvolution *Geophys. J. Int.* **178** 1649–62
- Ranieri G, Haile T and Alemayehu T 2005 TEM-fast small-loop soundings to map underground tunnels and galleries connecting the rock-hewn churches of Lalibela, Ethiopia *Geoarchaeology* **20** 433–48
- Safar M H 1985 On the lateral resolution achieved by Kirchhoff migration *Geophysics* **50** 1091–9
- Snieder R, Sheiman J and Calvert R 2006 Equivalence of the virtual-source method and wave-field deconvolution in seismic interferometry *Phys. Rev. E* **73**
- Wu R S and Toksoz M N 1987 Diffraction tomography and multisource holograph applied to seismic imaging *Geophysics* **52** 11–25
- Xue G Q, Li X, Guo W B, Song J P and Di Q Y 2006 Equivalent transformation from TEM field sounding data to plane-wave electromagnetic sounding data *Chin. J. Geophys.* **49** 1539–45
- Xue G Q, Yan Y J and Li X 2007 Pseudo-seismic wavelet transformation of transient electromagnetic response in geophysical exploration *Geophys. Res. Lett.* **34** L16405